Assessment and Control of Spacecraft Charging Risks on the International Space Station

Steve Koontz*, Marybeth Edeen*, William Spetch*, Penni Dalton#, Thomas Keeping*

* NASA Johnson Space Center, Houston, Texas, USA
\# NASA Glenn Research Center, Cleveland, Ohio, USA

Abstract

Electrical interactions between the F2 region ionospheric plasma and the 160V photovoltaic (PV) electrical power system on the International Space Station (ISS) can produce floating potentials (FP) on ISS conducting structure of greater magnitude than are usually observed on spacecraft in low-Earth orbit. Flight through the geomagnetic field also causes magnetic induction charging of ISS conducting structure. Charging processes resulting from interaction of ISS with auroral electrons may also contribute to charging, albeit rarely. The magnitude and frequency of occurrence of possibly hazardous charging events depends on the ISS assembly stage (six more 160V PV arrays will be added to ISS), ISS flight configuration, ISS position (latitude and longitude), and the natural variability in the ionospheric flight environment. At present, ISS is equipped with two plasma contactors designed to control ISS FP to within 40 volts of the ambient F2 plasma.

The negative-polarity grounding scheme utilized in the ISS 160V power system leads, naturally, to negative values of ISS FP. A negative ISS structural FP leads to application of electrostatic fields across the dielectrics that separate conducting structure from the ambient F2 plasma, thereby enabling dielectric breakdown and arcing. Degradation of some thermal control coatings and noise in electrical systems can result. Continued review and evaluation of the putative charging hazards, as required by the ISS Program Office, revealed that ISS charging could produce a risk of electric shock to the ISS crew during extra vehicular activity.

ISS charging risks are being evaluated in ongoing ISS charging measurements and analysis campaigns. The results of ISS charging measurements are combined with a recently developed detailed model of the ISS charging process and an extensive analysis of historical ionospheric variability data, to assess ISS charging risks using Probabilistic Risk Assessment (PRA) methods. The PRA analysis (estimated frequency of occurrence and severity of the charging hazards) are then used to select the hazard control strategy that provides the best overall safety and mission success environment for ISS and the ISS crew. This paper presents: 1) a summary of ISS spacecraft charging analysis, measurements, observations made to date, 2) plans for future ISS spacecraft charging measurement campaigns, and 3) a detailed discussion of the PRA

strategy used to assess ISS spacecraft charging risks and select charging hazard control strategies

High-Voltage Photovoltaic Array and Magnetic Induction Driven Charging

The relatively high plasma density, low plasma temperature, and high electrical conductivity characteristic of the F2 region ionospheric plasma preclude many of the spacecraft charging processes that are observed in lower density plasma environments (1,2,7). Surprisingly, the most important identified spacecraft charging process for ISS requires a high-density, low-temperature plasma environment. An electrical interaction between the F2 plasma and the 160-V US PV arrays can produce an electrical potential difference between the conducting structure of ISS and the ambient plasma (i.e. a floating potential or FP) much greater than that usually observed for spacecraft in low-Earth orbit (LEO), most of which have 28-V PV array power systems (7-12). Sky Lab, which employed 90-V PV arrays, is an important exception to be discussed below. As is shown below, ISS conducting structure becomes negatively charged with respect to the ambient plasma because the PV arrays and electrical power system utilize a negative-polarity grounding scheme, and the common ground point is ISS conducting structure. The severity of possible charging hazards is determined by materials and configuration interactions with the F2 plasma environment (7-12).

Spacecraft charging interactions lead to the application of electrostatic fields across the dielectrics that separate conducting structure from the ambient F2 plasma. The magnitude of the field gradient can be large enough to cause dielectric breakdown and arcing (7-12). Degradation of some thermal control coatings, electrical system noise, and shock hazards to extra-vehicular activity (EVA) crew may result (7-12) if the FP is sufficiently negative. The following simple calculation is aimed at explaining the PV array driven charging process, while highlighting the important role of materials-environment interactions in both the charging process and the subsequent analysis of possible hazards.

The physical basis of PV array driven spacecraft charging lies in the fact that the ions and electrons in the F2 plasma have nearly the same gas kinetic temperature and, therefore, nearly the same kinetic energy. Because the electrons are much less massive than the ions ($m_i >> m_e$), the mean gas-kinetic speed for electrons, $v_e = \sqrt{(8kT_e/2\pi m_e)}$, is much larger than the mean gas kinetic speed for the ions, $v_i = \sqrt{(8kT_i/2\pi m_i)}$. Therefore, the flux of electrons (electron current, I^-) to any surface is much greater than the flux of ions (ion current, I^+) until a steady state negative FP is established such that $I^+ + I^- = 0$.

Each of the 400 photovoltaic cells in one string of the US PV array produces about 0.4 V in sunlight, yielding a total linear ΔV of 160 V from one end of the string to the other. There are 82 strings per PV array wing. In the real PV array, the string is mounted on one side of an insulating flat plate of length L (same as the string length). The plate is flying through the ionosphere at orbital velocity with the PV array string facing forward (ram orientation). The FP can be calculated point by point along the string given ΔV, orbital velocity (v_{ISS}), the electron and ion densities (Ne and Ni) and the corresponding gas kinetic temperatures, Te and Ti, in the F2 plasma. Geomagnetic

field effects on current collection from the F2 plasma are small enough to neglect for this analysis. Orbit limited current collection, electrostatic focusing effects (1,2), and detailed PV array lay-out are also neglected, for the sake of simplicity, even though the subject effects are large and lead to smaller measured values of ISS FP than were predicted by simple early treatments (9).

The thermal velocity of the plasma ions, v_i, is much less than orbital velocity of the spacecraft, v_{ISS}, so that only ram ion collection is considered. In contrast, the thermal speed of the plasma electrons is much greater than orbital velocity so that electron collection is by gas-kinetic diffusion to the Debye sheath (1,2) and then to the collecting surface. The faster electrons cannot catch up with the spacecraft from behind because separation from the slower moving ions in the wake region creates an opposing electric field (ambipolar diffusion (1,2). As a result, simply turning the PV array strings to wake and exposing only the insulating plate to ram completely suppresses PV array driven charging, a prediction confirmed by in-flight ISS floating potential and plasma contactor emission current measurements made during 2001 (15,16). Finally, the magnitude of the charging depends on the PV array voltage. When ΔV is zero, at night or when the PV strings are shunted, there is no charging.

At steady state, plasma ion current to the string must equal plasma electron current to the string.

$$\text{Electron thermal current} = I^- = I^+ = \text{Ion ram current}$$

The positively biased end (area A_e, length L_e) of the string collects electrons and the negatively biased end (area A_i, length L_i) collects ions. $A_e + A_i = A$, and $L_e + L_i = L$, where A is the total exposed conducting area on the PV cell string of length L.

$$I^- = 0.25 v_e N_e q A_e = v_{ISS} N_i q A_i = I^+.$$

The ionosphere is a neutral plasma so, $N_e = N_i$. The mean gas-kinetic speed of the electrons, v_e, is multiplied by 0.25 to obtain the correct expression for thermal particle flux to a wall, and q is the value of the elementary charge leading to,

$$0.25 v_e A_e = v_i A_i \text{ or } A_e/A_i = v_{ISS}/0.25 v_e$$

Assuming a typical daytime F2 region plasma temperature of 0.1 eV (1,160° K) we have $v_i = 1.3$ km/sec, $v_{ISS} = 7.69$km/sec, and $v_e = 163$ km/sec so that,

$$A_e/A_i = v_{ISS}/0.25 v_e = (7.69)/(0.25 \times 163) = 0.19.$$

Since PV string voltage is a linear function of distance from the positive end, and $\Delta V = 160$ V, FP can now be calculated as a function of distance from the positive end of the string, where FP(0) corresponds to L=0.

$$FP(0) = \Delta V(A_e)/(A_i+A_e) = \Delta V(L_e)/(L_i+L_e) = 160 \times 0.1597 = +26 \text{ volts}$$

$$FP(L) = FP(0) - \Delta V = -134 \text{ V}$$

If the negative end of the string is grounded to a spherical conducting structure that is 10 meters in radius (a reasonable size compared to ISS pressurized elements), the free space capacitance ($C_{fs} = 4\pi\varepsilon\varepsilon_o r = 1112$ pF; ε = dielectric constant, ε_o= free space permittivity) of the structure is charged to –134 volts giving a stored energy of only $E = 0.5CV^2 = 10$ micro Joules.

Covering the sphere with a thin dielectric surface coating changes the character of the charging hazard dramatically. On the ram facing side of the sphere, the FP of the external surface of the dielectric film will approach 0 V as a result of positive charge collection from the ionosphere, and –134 V is applied across the dielectric. Now the sphere is best described as a parallel plate capacitor (the conducting structure is one plate and the conducting ionosphere is the other) able to store energy

$$E = 0.5\ CV^2 = 0.5\ \varepsilon\varepsilon_o(A_{ram}/d)V^2 = (0.5)(8.85 \times 10^{-12})\varepsilon(2\pi r^2/d)\ V^2,$$

where A_{ram} is the area of the hemisphere able to collect positive charge from the ionosphere. If d is 1 micron (1.3 microns is the thickness of the anodic coating on the US Lab and Node 1 meteoroid and debris shields) and $\varepsilon = 5$ for aluminum oxide, the stored energy becomes E = 250 Joules. Now, dielectric breakdown of the thin surface coating can discharge the parallel plate capacitor, releasing enough energy to damage the dielectric coating itself and producing enough voltage and current to present a possibly lethal hazard to any EVA crew in the discharge circuit. The high-density, low-resistance dielectric-breakdown arc plasma provides the conductive path connecting the negatively charged conducting structure to the positively charged dielectric film surface (8-10).

Note that the stored energy is inversely proportional to the dielectric film thickness. Simply increasing the film thickness from 1.0 micron to 100 microns reduces the stored energy from 249.5 Joules to 2.49 Joules while greatly reducing the risk of dielectric breakdown arcing. The thick (>120 microns) dielectric coatings on Sky Lab minimized any charging hazards that might have been generated by the 90-V PV array on that spacecraft. Similarly, the Russian elements of ISS contribute little to the charging hazard because surface dielectric coatings are thick. Stored energy is also directly proportional to V^2, and reducing the FP at the negative end of the PV array to –40V reduces the stored energy to 0.9 micro Joules for the uncoated conducting sphere, and 22 Joules for the dielectric coated sphere. As discussed below, flight measurement and analysis of US Lab and Node 1 FP, with all FP controls disabled and PV array driven charging enabled, have not exceeded –28 volts during 2001 (16). Plasma chamber testing (7-12) has shown that the dielectric breakdown voltage for the 1.3-micron thick anodic film on the US Lab and Node 1 meteoroid and debris shields is greater than 60 volts. Therefore, the plasma contactor system has not been in continuous operation since May 2001. The ISS FP not-to-exceed-limit for EVA safety is –40 V, however and two PCUs are operated routinely during EVA.

A negative FP of –134 V is remarkably close to the predictions made before the US PV arrays were flown for the first time on ISS (7-10). Using early charging models, a worst-case FP of –140 volts was predicted. The measured FP from PV array driven

charging on ISS have been less negative than –28 V in all cases observed to date. The simple charging calculation presented above as well as the more elaborate pre-flight theoretical models consider only current collection by the PV array string. Ion collection by exposed conducting structure attached to the negative end of the PV array string can offset the effects of electron collection by the string, driving FP(0) toward +160V and FP(L) toward 0 volts, but only if the number of milliamps of electron current collected by the PV array is small. The number of square meters of ram-oriented ion-collecting surface needed to hold the PV array FP (0) near +150 V and FP(L) near -10 volts is shown as a function of total electron current collected by the PV arrays in Table 1.

Table 1: Area of Exposed Conducting Materials Compensating PV Array Electron Collection *

Ionospheric Electron Current Collected by 160 V PV Arrays (milliamps)	Area of Ram Oriented Ion Collection Surface (square meters)
10	8
30	24
60	48
100	80

*** FP (0) =+150 V and FP (L) = -10 V; Ni = Ne =10^6/cc**

When the electron current collected by the PV arrays on an LEO spacecraft is less than about 60 milliamps, exposed ion conducting area connected to the negative ground plane can offer practical FP control. As the collected electron current grows beyond 100 milliamps, the ion collecting area requirements become unrealistic. The plasma contactor system was selected for ISS FP control precisely because the magnitude of the electron current collected from the ionosphere by the 160-V US PV arrays was estimated to be far too large to allow FP control by passive ion collection surfaces (9, 14). The Russian segment of ISS provides significant ram-oriented conducting surface area (estimated to be greater than 30 square meters) as a result of Russian Program electrical conductivity/grounding requirements for thermal blanket materials.

The plasma contactor system on ISS controls the FP by providing a low impedance return path to the ionosphere for electrons collected by the PV arrays or by other collection mechanisms (17). The ISS telemetry stream provides measurements of electron emission current from the ISS ground plane to the ionosphere whenever the plasma contactor system is operating. Much of the plasma contactor emission current observed over the past 2 years is attributable to low-voltage non-PV-array-driven charging processes (17). However, direct measurements of PV array driven electron collection can be made by recording the change in emission current when ISS enters sunlight (eclipse exit) with sun-pointing PV arrays or by shunting and un-shunting the sun-pointing PV arrays while in sunlight.

Figure 1 shows measured eclipse-exit plasma contactor emission currents since January 2001. The eclipse exit emission currents show considerable variation both during a given 24-hour day and over the last year. The well-known dynamic structure of the F2 region of the ionosphere (1,2) can account much of the variability. Large variations of Ne and Te with time of day, altitude, ISS latitude and longitude, geomagnetic field, solar activity, and season explain much of the observed variability in the eclipse exit

emission currents (1,2,18). Clearly, the magnitude of PV-array-driven charging will vary in a similar way with variation in natural environment.

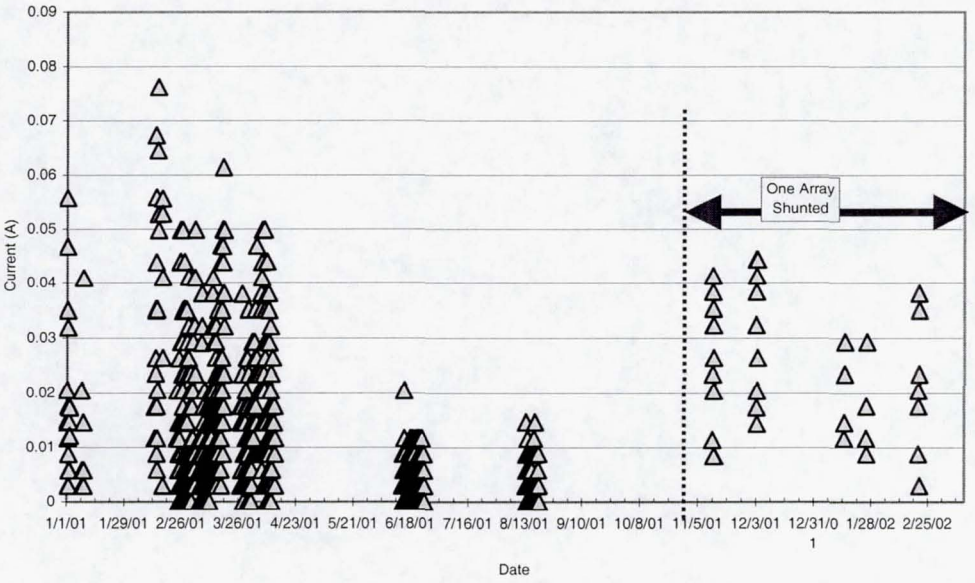

Figure 1. ISS plasma contactor emission current increase at eclipse exit; Jan 2001 to Feb 2002, US 160 V PV arrays sun tracking and un-shunted

With the plasma contactors operating, most of the PV array wing area is positively biased (+FP) so that electron collection is maximized and any ion collection by conducting structure is already accounted for in the observed emission currents. If the plasma contactors are turned off, the FP at the negative end of the PV array (and ISS conducting structure) moves toward more negative values. As a result, less of the PV array wing area is positively biased leading to reduced electron collection, while ion collection remains constant or increases slightly. At some negative value of the conducting structure FP, PV array electron collection will equal conducting structure ion collection stopping further movement of FP toward more negative values.

In the simple flat-plate charging calculation shown above, the reduction in PV array electron collection is a simple linear function of FP at the negative end of the array. In fact, as FP becomes more negative, the decrease in electron collection by the PV arrays is nonlinear as a result of: 1) dielectric surface charging of PV array cell materials, 2) detailed electrostatic focusing effects in the Debye sheath near the gap between PV array cells, and 3) PV array cell structure and lay-out. Small negative changes in FP cause relatively large reductions in electron collection while ion collection remains nearly constant (9b, 9c, 18). Steady state FP values with the plasma contactor system off are expected to be less than –40 Volts, not –134 Volts, as has been observed to date (15,16,18). As development of more accurate and detailed models of the PV array driven charging process continues, it becomes clear that a materials interaction with the

ionospheric environment, specifically surface charging of dielectric materials in the photovoltaic cell structure, limits electron collection by the 160 V US PV arrays on ISS and places natural limits on the FP values that can be achieved (18), though frequency of occurrence and magnitude of the negative FP is expected to increase as more PV array wings are added to ISS.

The results of in-flight floating potential probe (FPP) (15,16) measurements of ISS FP characterizing both the PV array driven charging process and the contribution of the **vxB·L** (**v** = spacecraft velocity, **B** = geomagnetic field, **L** = length of conducting structure) magnetic induction voltages, with the plasma contactor system off, are shown in Figure 2 and Tables 2 and 3.

Table 2 compares the worst-case pre-flight predictions of PV array driven charging with the worst-case measurement made to data. Measured electron collection by the two 160-V US PV arrays active during the April 2001 time frame is so low that exposed conducting structure can contribute to limiting the negative FP to the small value observed, as suggested above.

FPP measurements of ISS FP were made during several days in 2001, including intervals when the Space Shuttle was docked to ISS. On January 31, FPP data measurements of ISS FP were made with active side (the side with PV cell strings) of the active surface of the PV arrays in shallow wake flight attitude verifying that wake orientation of the arrays prevents PV array driven charging.

With the plasma contactor system off and PV arrays sun tracking, FPP data was collected on April 10-12, April 15, and on April 21 (before and after Space Shuttle docking). A total of 46 FP measurements characterizing PV array driven charging were made in 2001, encompassing a wide range of ionospheric conditions. Langmuir probe measurements of electron temperature, Te, at eclipse exit ranged from 0.08 to 0.23 eV while electron density, Ne, ranged from 10^9 to $10^{12}/m^3$. To date, the observed range of PV array-driven charging FP values range from –4 to –24 V. It should be noted that the FPP could not provide Te or Ne if Fp exceeded –10V negative as a result of the limited sweep range of the Langmuir probe voltage.

The April 11 data is fairly typical, despite the geomagnetic storm starting about 13:30 universal time (UT). Figure 2 shows the ISS FP at the FPP measurement point as a function of universal time on April 11, 2001. In Table 3 the total FP for the April 11, 2001 eclipse-exit charging peaks, shown in Figure 2, are broken down into the magnetic induction and PV array driven components for the locations on ISS defined in Figure 3.

Magnetic induction voltage is a significant fraction of the total FP in all cases, and must be considered in any ISS charging assessment. As shown in Figure 2, the agreement between calculated magnetic induction voltage and measurement is excellent in all cases. Figure 3 shows a calculated magnetic induction voltage map of ISS when passing south of Australia on April 11, 2001. Flight south of Australia generates the more magnetic induction voltage on ISS than any other ISS flight path.

Table 2: PV Array Driven Charging - Pre-Flight Estimates vs. Flight Data

Charging Hazard Related Quantity	Pre ISS Flight 4A: Worst-Case Estimate	Post Flight 4A: Worst-Case at US Lab Module
Maximum Negative FP	-140	-26 V
160 V PV Array Electron Collection	200 to 500 milliamps	10 to 80 milliamps
Exposed Conducting Surfaces on ISS	0 m^2	15 to 40m^2: PV array mast wires & ISS structure
Duration of Max. Neg. FP	20 to 30 min. of day pass	<10 min. of day pass

The data shown in Figure 2 and Table 3 span 6 orbits or 9 hours. During that time, the rotation of the Earth changed the geographic location of ISS eclipse exit from near the west coast of South America to Australia. The magnetic induction voltage peaks twice on each orbit, at $\pm$ 51.6 degrees latitude. Eclipse-exit PV array driven charging peaks are superimposed on the –51.6 latitude magnetic induction peaks. The + 51.6 magnetic induction voltage peak occurs during eclipse. The measured FP consists only of magnetic induction during voltage when ISS is in eclipse or when the PV arrays are shunted or in wake. When sun tracking, the active surface of the PV arrays move into wake at orbital noon. Figure 2 also shows a comparison of magnetic induction voltages calculated using a first principle model (17,18) with the flight data, demonstrating excellent agreement between the magnetic induction model and the flight data. The ISS magnetic induction voltage map shown in Figure 3 was calculated using the model (17, 18).

Table 3: Post Eclipse Exit ISS Charging Peaks (maximum negative FP in volts) from Figure 2, April 11, 2001 at GMT time indicated (PCU system off)

12:38	2B	LAB	FPP	4B
vxB	2.034	-6.51	-3.42	-9.56
Chg	-19.6	-19.6	-19.6	-19.6
Total	-17.5	-26.1	-23.0	-29.1

14:10	2B	LAB	FPP	4B
vxB	2.571	-7.38	-4.19	-11.5
Chg	-17.0	-17.0	-17.0	-17.0
Total	-14.4	-24.4	-21.2	-28.5

15:41	2B	LAB	FPP	4B
vxB	2.812	-8.22	-4.96	-13.5
Chg	-15.2	-15.2	-15.2	-15.2
Total	-12.4	-23.5	-20.2	-28.7

17:15	2B	LAB	FPP	4B
vxB	3.429	-9.7	-6.55	-17.2
Chg	-7.0	-7.0	-7.0	-7.0
Total	-3.5	-16.7	-13.5	-24.2

18:46	2B	LAB	FPP	4B
vxB	3.775	-10.2	-7.35	-19.1
Chg	-4.7	-4.7	-4.7	-4.7
Total	-0.9	-14.9	-12.0	-23.8

20:18	2B	LAB	FPP	4B
vxB	3.903	-10.1	-7.65	-19.7
Chg	-5.2	-5.2	-5.2	-5.2
Total	-1.3	-15.3	-12.9	-25.0

Table 3 definitions: vxB=magnetic induction voltage; Chg=PV array driven charging; Total=vxB + Chg; For ISS locations 2B, 4B, Lab and FPP see figure 3

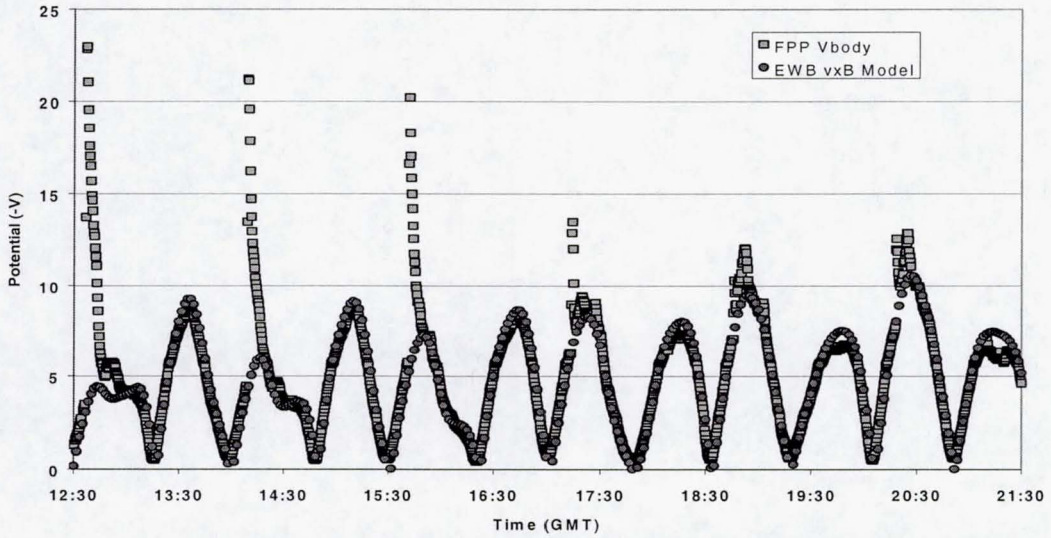

Figure 2: ISS FP at the FPP measurement point (FPP Vbody) with the plasma contactor system off. Calculated magnetic induction FP (EWB vxB model) is compared with measured FP. April 11, 2001

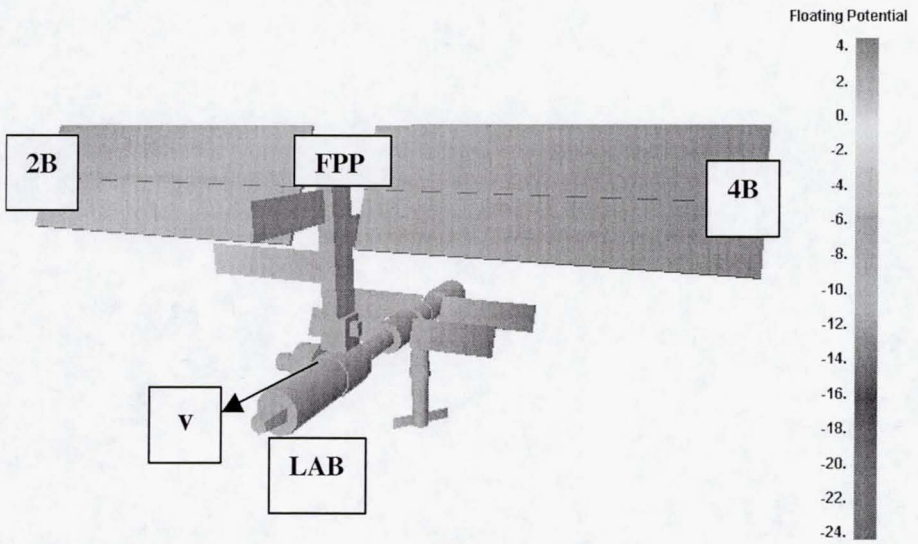

Figure 3: Calculated worst-case magnetic induction voltage map of ISS in +XVV flight attitude (velocity vector v), with 10 degrees down pitch. April 11, 2001

The ISS Program has established a process for the evaluation and management of spacecraft charging processes on ISS and has established a requirement for control of ISS FP to values less negative than –40V during EVA operations for all EVA work sites and translation paths. The plasma contactor system (11-13) provides the primary control of ISS floating potential. Shunting the PV arrays or orienting the active surfaces of the PV arrays to wake are additional FP control methods verified for the present ISS flight configuration.

As the ISS construction continues, six more 160 V US PV array wings will be added along with the complete truss structure and additional Russian, European, and Japanese modules. Adding six PV array wings increases the risk from PV array driven charging and the completed ISS truss is long enough to develop worst-case tip-to-tip magnetic induction voltages of –50 V. In-flight characterization of ISS floating potentials, and local ionospheric environment are essential for verification of a safe EVA environment as construction of ISS continues. A dedicated floating potential measurement unit (FPMU) will be installed on ISS before the next set of 160 V PV arrays is launched. The FPMU consists of a floating potential probe, two Langmuir probes, and a plasma impedance probe. Langmuir probe measurements will be verified against ground based incoherent scatter radar and ionosonde data. Measurement campaigns are planned to fully characterize the ISS charging and EVA shock hazard environment, verify the effectiveness of hazard controls, and verify the detailed ISS charging models (18).

High Latitude Auroral Electron Charging

The possibility of spacecraft charging by auroral electrons at high latitudes, during geomagnetic storms or other geomagnetic disturbances, is a subject of some concern on the part of the spacecraft charging community (20, 22-24). Analysis of historical satellite charging and anomaly data for the United States Defense Meteorological Satellite Program (DMSP) satellites and the European Space Agency Freja satellite both suggest that auroral charging may be observed on ISS at high magnetic latitudes (25, 26), especially at night during solar minimum. Charging of the Freja and DMSP vehicles has been correlated with ionospheric plasma densities of $10^4/cm^2$, or less, combined with fluxes of energetic auroral electrons (7-10 keV) greater than 10^8 electrons/(cm^2sec sr) (23, 26-28). The DMSP and Freja satellites both orbit the Earth at or above 800 km, in the topside ionosphere, well above ISS operational altitudes. Nonetheless, the required combinations of ionospheric plasma density and energetic electron flux are expected to occur at ISS altitudes, albeit infrequently, at or near the extreme latitudes of the ISS orbit ($\pm$ 51.6°). Inspection of the auroral precipitation maps produced hourly by the US National Oceanics and Atmospherics Administration (NOAA) Polar Orbiting Environmental Satellite (POES) constellation show that ISS passes through the precipitating auroral electrons several times every day, whenever ISS passes south of Australia at night and Kp is greater than 3 (29).

The question of whether or not flight through the same kind of environment that produces charging and the occasional recoverable anomaly on DMSP constitute a risk or hazard for ISS or ISS EVA crew remains open. The absence of severe anomalies on the Freja spacecraft in a similar, if not more severe, charging environment highlight the important effect of spacecraft design on spacecraft charging. More detailed

assessments of the frequency of occurrence of the auroral charging environment at 350 to 400 km altitude as well as detailed analysis and modeling of the expected ISS and EVA suit charging in that environment are in work at this time. ISS and the EVA suits used on ISS are not identical to DMSP or Freja, when treated as electrical systems interacting with the auroral charging environment. Materials properties and materials interactions with the auroral charging environment will likely determine the outcome of the assessments. Secondary electron yields, dielectric coating thickness compared to energetic electron range, and total area of exposed conducting surfaces are all important factors. The ISS plasma contactor system also contributes to control of any auroral charging risk by both increasing local plasma density and providing a return path to the ionosphere for any charging of ISS grounded structure produced by auroral electrons.

During the first two years of flight (during the current solar maximum), no ISS equipment anomalies have been reported that correlate with geomagnetic storms or flight through either the diffuse or visible auroras. The ISS crews have reported flying through visible Aurora Australis on at least two occasions. The following excerpt from Commander William Shepherd's deck log of Nov. 10, 2000 is an interesting example.

"11:30: Transited through a very unusual aurora field. Started as a faint green cloud on the horizon, which grew stronger as we approached. Aurora filled our view field from SM (Service Module) nadir ports as we flew through it. A faint reddish plasma layer was above the green field and topped out higher than our orbital altitude."

Southern hemisphere auroral precipitation maps produced by NOAA POES Satellites 15 (Nov. 10, 2000 10:56 UT) and 16(Nov. 10, 2000 12:26 UT) show auroral activity levels of 9, hemispheric powers of 60 to 90 gigawatts, with intense auroral electron precipitation over Tasmania and southern New Zealand, so that ISS was well within the precipitating electron environment during the auroral fly through reported by Cmdr. Shepherd (17).

References

1) NASA Technical Memorandum 4527; Natural Orbital Environment Guidelines for Use in Aerospace Vehicle Development; Anderson, Jeffery B., Editor; Smith, Robert E., Compiler; June 1994; and Lieberman, M. A., Lichtenberg, A. J.; Principles of Plasma Discharges and Materials Processing, John Wiley and Sons Inc., New York, 1994
2) Handbook of Geophysics and the Space Environment; Jursa, Adolph S., Editor, Air Force Geophysics Laboratory, Air Force Systems Command, United States Air Force, 1985
3) Garrett, H. B., Whittlesey, A. C.; "Spacecraft Charging, An Update," AIAA 96-0143, 34th AIAA Aerospace Sciences Meeting and Exhibit, 15-18, January 1996, Reno Nevada
4) Vaughn, J.A., Carruth, M. R., Katz, I., Mandell, M., Jongeward, G. A.; "Electrical Breakdown Currents on Large Spacecraft in Low Earth Orbit," J. Spacecraft and Rockets, Vol. 31, No. 1, January-February 1994, pp 54-59
5) a) Snyder, David B.; "Dynamic Interactions Between Ionospheric Plasma and Spacecraft," The Radio Science Bulletin, No. 274, Sept, 1995, pp 29-36, b) Ferguson, D. C., Hillard, G. B.; "In Space Measurement of Electron Current Collection by Space Station Solar Arrays," AIAA 95-0486, 33rd Aerospace Sciences Meeting and Exhibit, January 9-12, 1995, Reno NV., c) de la Cruz, C. P., Hastings, D. E., Ferguson, D., Hillard, B.;"Data analysis and model comparison for solar

Array Module Plasma Interactions Experiment," J. Spacecraft and Rockets, Vol.. 33, No. 3, pp 438-446, May-June 1996, d) Hastings, D. E., Cho, M., Kuninaka, H., "The Arcing Rate for a High Voltage Solar Array," Journal of spacecraft and Rockets, 29, No.4, 538-554, 1992, e) Hastings, D. E.; "A Review of Plasma Interactions with spacecraft in Low Earth Orbit," Journal of Geophysical Research, 100, No. A8, PP. 14457-14484, 1995

6) Galofaro, J. T., Doreswaamy, C. V., Vayner, B. V., Snyder, D. B., Ferguson, D. C.; "Electrical Breakdown of anodized Structures in a Low Earth Orbit Environment," NASA/TM – 1999-209044, April, 1999
7) Vayner, B. V., Galofarno, J., Ferguson, D. C., de Groot, W., Thompson, C., Dennison, J. R., Davis, R.; "The Conductor- Dielectric Junctions in a Low Density Plasma," NASA/TM – 1999-209408, Nov. 1999
8) Murphy, G., Croley, D., Ratliff, M., Leung, P.; "The Role of External Circuit Impedance in Dielectric Breakdown," AIAA 92-0821, 30th Aerospace Scoiences Meeting and Exhibit, Jan. 6-9, 1992/Reno, NV
9) Patterson, M. J., Verhey, T. R., Soulas, G., Zakany, J.; " Space Station Cathode Design Performance and Operating Specifications," IEPC Paper Number 97-170, 25th International Electric Propulsion Conference, Cleveland Ohio, Aug. 1997.
10) Lambert, J. C., Chaky, R. C.; "The ISS Plasma Contactor," AIAA 96-0627, 34th Aerospace Sciences Meeting, Jan. 15-18, 1996, Reno NV.
11) Ferguson, D. C., Morton, T. L., Hillard, B. G.; "First Results from the Floating Potential Probe (FPP) on International Space Station," AIAA-2001-0402, 39th Aerospace Sciences Meeting and Exhibit, Jan. 2001, Reno, Nevada
12) Morton, Tl L., Minow, J. I.; "Floating Potential Langmuir Probe Data Reduction Results," AIAA-2002-0936, 40th AIAA Aerospace Sciences Meeting and Exhibit, 14-17, January 2002, Reno Nevada
13) Bering, E. A., Koontz, S., Katz, I., Gardner, B., Evans, D., Ferguson, D.; "The Plasma Environment of the International Space Station in the Austral Summer Auroral Zone Inferred from Plasma Contactor Data," AIAA 0220-0935, 40th AIAA Aerospace Sciences Meeting and Exhibit, 14-17, January 2002, Reno Nevada
14) Mikatarian, R.R., Kern, J.W., Barsamian, H.R. and Koontz, S.L., "Plasma Charging of the International Space Station", to be presented at the COSPAR World Space Congress, Houston, Texas, October 2002
15) Katz, I., Lilley, J. R., Greb, A., McCoy, J. E., Galofaro, J., Ferguson, D. C.; "Plasma turbulence enhanced current collection: Results form the plasma motor generator electrodynamic tether flight," J. Geohys. Res., Vol. 100, No. A2, pp1687-1690, Feb. 1, 1995
16) Stone, N. H.; "The Aerodynamics of Bodies in a Rarefied Ionized Gas with Applications to Spacecraft Environmental Dynamics," NASA Technical Paper 1933, November 1981
17) Martin, A. R.; "Spacecraft/Plasma Interactions and Electromagnetic Effects in LEO and Polar Orbits," Final Report for ESA/ESTEC Contract Number 7989/88/NL/PB(SC), Vol. 3, 1991
18) Personal Communication, William Spetch, Vehicle Integrated Performance Engineering (VIPeR) Office, Mail Code OM, NASA Johnson Space Center, Houston, Texas 77058
19) Minow, J. I., Neergaard, L. F., Maurits, S., Hwang, K., Suggs, R. M.; "High Latitude Plasma Electrodynamics and Spacecraft Charging in Low-Earth Orbit," ESA/SCTC, 23-27, April, 2001
20) Purvis, C. K., Snyder, D. B., Jongeward, G. A.; "Auroral Interactions with ISSA," NASA Technical Memorandum 106794, December 1994
21) Cooke, D. L.; "Simulation of an Auroral Charging Anomaly on the DMSP Satellite," 6th Spacecraft Charging Technology Conference, AFRL-VS-TR-20001578, 1 Sept., 2000
22) Gussenhoven M. S., Hardy, D. A., Rich, F., Burke, W. J.; Yeh, H-C.; "High-Level Spacecraft Charging in the Low-Altitude Polar Auroral Environment," Journal of Geophysical Research, Vol. 90, NO. A11, 11,009-11-023, November 1985
23) Wahlund, J-E., Wedin, L. J., Carrozi, T., Eriksson, A. I., Holback, B. Anderson, L., Laakso, H.; "Analysis of Freja Charging Events: Statistical Occurrence of Charging Events," WP-130 Technical Note (SPEE-WP130-TN), Version 2.0, ESA contract 11974/96/NL/JG(SC), 22 February, 1999
24) Stevens, N. J., Jones, M. R.; "Comparison of Auroral Charging Predictions to DMSP Data," AIAA 95-0370, 33rd Aerospace Sciences Meeting and Exhibit, January 9-12, 1995, Reno NV.
25) http://www.sec.noaa.gov/pmap/